JMEPEG (2007) 16:163–169
DOI: 10.1007/s11665-007-9027-1

1059-9495/$19.00

Post-Processing Effect on the Fatigue Behavior of Three Titanium Alloys under Simulated SPF Conditions

F. Pitt and M. Ramulu

(Submitted April 20, 2006; in revised form October 22, 2006)

This experimental study investigates a post-Superplastic Forming (SPF) processing method with reduced material removal requirements and its effect on high-cycle fatigue behavior. Comprehensive high-cycle fatigue experiments were conducted on three titanium alloys in part to validate the proposed post process and in part to provide baseline properties for evaluating additional materials. High-Cycle Fatigue results indicated that lower temperature superplastic forming conditions allow more efficient use of titanium material. Manufacturing process designers needing to predict the best SPF conditions and establish design allowables for titanium alloys may find the results of this research useful.

Keywords alpha case, high-cycle fatigue, superplastic forming, surface roughness, titanium alloy

1. Introduction

Aerospace materials today include an increasing quantity of titanium alloys. As operating temperatures increase, fuel efficiency becomes more important and corrosion issues receive more attention, titanium alloys become more cost effective. Reducing the cost of titanium structure will allow its benefits to be applied even further.

Superplastic Forming (SPF) is a relatively new sheet metal manufacturing process, becoming popular in the 1960s, and is utilized primarily to fabricate titanium sheet metal parts. During the SPF process, which involves heating the titanium in air, oxygen diffuses interstitially into the titanium material and forms a hardened, brittle layer known as α case (Ref 1). The most dramatic effect of α case and interstitial contamination is the reduction of high-cycle fatigue properties (Ref 2). To date, removal of the α case layer has been the method of choice for restoring the ductility after SPF in aerospace parts.

Titanium material with α case has been known to fail in fatigue at less than half of the life of titanium material without α case (Ref 3). The curve of the stretched material with α case removed (square markers) compared to the curve of the material stretched with α case not removed (star markers) in Fig. 1 clearly illustrates this drop in fatigue life. Comparing the results at a life of 4×10^4 cycles, exposure to SPF conditions reduces the maximum stress by 23%. Removal of the α case layer restores the stress capability to within 11% of the unprocessed material. Figure 2 contains a micrograph showing surface cracks in the α case on a section of titanium material following temperature exposure only.

High-cycle fatigue (S-N) experiments in titanium produce important data for evaluating materials with respect to service life in aircraft structures. Titanium alloys are very sensitive to surface defects and flaws, including surface roughness, that affect crack initiation. Therefore the S-N evaluation is valuable in evaluating different methods and processes that could affect the surface of the titanium.

2. Experimental Method

Three alloys of titanium were evaluated during the experimental portion of this evaluation. Nominal and measured alloy chemistries are shown in Table 1. Mill annealed sheet titanium of each alloy was fabricated into full thickness test specimens prior to being exposed to simulated SPF conditions as shown in the third row of Table 2. Following the simulated SPF conditioning, the specimens were subjected to one of the three post-processing methods (AE, PP, FP), also described in Table 2.

The S-N evaluation is the definitive test for determining the effect of simulated SPF exposure on these three titanium alloys with respect to performance in aerospace applications. The high cycle, constant amplitude, stress controlled fatigue test was conducted according to ASTM E 466-96. The sheet metal specimens are flat and have as-fabricated faces and machined edges with dimensions as shown in Fig. 3. Special care was taken in finishing the machined specimens so that the final material was removed with longitudinal strokes. These tests were conducted using a sinusoidal forcing function at 25 Hz, a K_t of 1.03, R of 0.1. Three similar MTS Test Star 2 fatigue testing systems were used to conduct, control, and monitor the tests, one system for each of the three titanium materials.

This article was presented at the AeroMat Conference, International Symposium on Superplasticity and Superplastic Forming (SPF) held in Seattle, WA, June 6-9, 2005

F. Pitt and **M. Ramulu,** Department of Mechanical Engineering, University of Washington, Box 352600 Seattle, WA 98195; and **F. Pitt,** The Boeing Company, Box 3707 Seattle, WA 98124. Contact e-mail: franna.s.pitt@boeing.com.

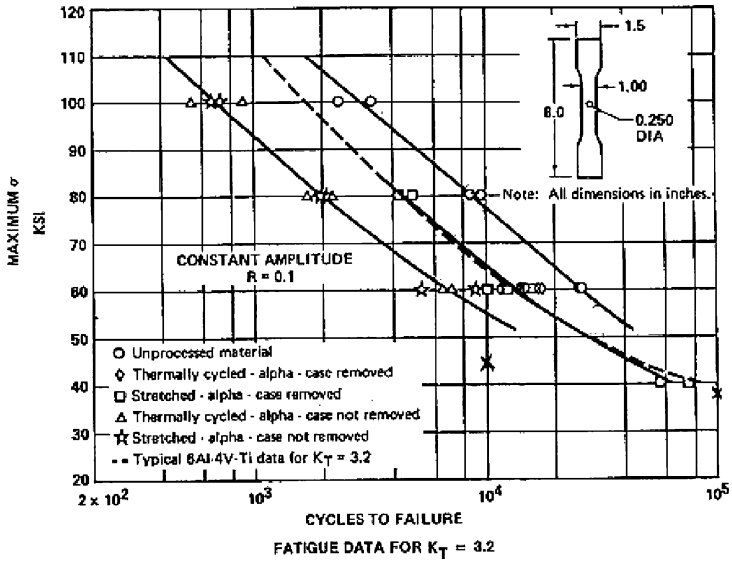

Fig. 1 Example S-N Fatigue Data for Ti 6Al-4V after SPF (Ref 3)

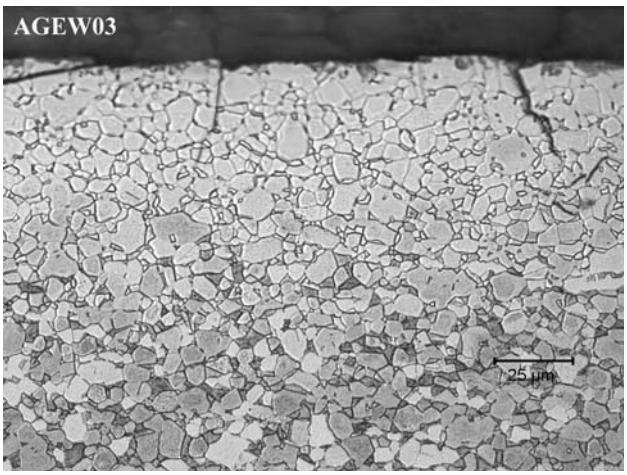

Fig. 2 Typical Titanium Micrograph showing pre-existing Cracks in the Alpha Case

Surface roughness was investigated as a potential cause for reduced fatigue life. The surface roughness was measured in four different locations, two transverse and two longitudinal, on one specimen from each of the four exposure/material groups. A Federal Surfanalyzer model EAS-4400-W1 and the 5-µm stylus probe was utilized to record the surface profiles. Average surface roughness (Ra), was determined from the surface profile of each of the four combinations of alloy and temperature conditioning.

Selected specimens were examined by visual and Scanning Electron Microscopy (SEM) using a Nikon macroscope, a Bausch and Lomb hand held 7X lens and the JEOL Scanning Electron Microscope.

3. Results

The results of the relationship between surface roughness and directional dependency in Ti 6-4 alloy showed that, for AR material, the transverse direction (T-direction) was rougher than the longitudinal direction (L-direction). Since the hot rolling process is involved in manufacturing sheet product, and stretches the material in the L-direction, it induces increased roughness in the T-direction by a factor of 2.3 for Ti 6-4. However, after the simulated SPF process the directional dependency is reduced. After conditioning to the 885 °C (1625 °F) cycle, Ti 6-4 shows a difference in surface roughness of less than 30% and is still a little bit rougher in the T-direction. The Ti 6-4 conditioned to the lower temperature (A4E) condition exhibits greater roughness in the T-direction by a factor of 1.8. On the other hand, the simulated SPF process induced rougher surfaces than the as received condition by a factor of 2 or more. The higher exposure temperature further increased the surface roughness. This implies that the thermal

Table 1 Titanium sheet material composition

	Weight % by inductively coupled plasma spectroscopy								
Alloy chemistry	**Al**	**V**	**Mo**	**Sn**	**Zr**	**Cr**	**Si**	**Fe**	**O%[a]**
Ti 6Al-4V (Ti 6-4)	6.25	4.23						0.2	0.160
Ti 6Al-2Mo-2Sn-2Zr-2Cr (Ti 6Q2)	5.93		2.05	2.12	2.14	1.04	0.23	0.03	0.107
Ti 5Al-3V-2Mo-2Fe (SP 700)	4.65	3.23	2.09					2.11	0.087

[a] Oxygen % determined using LECO TC-126 Oxygen/Nitrogen Determinator

Table 2 Simulated SPF processing conditions and definition

Condition	Description
AR	As Received, Mill Annealed
AR + CM	AR with 0.127 mm (0.005″) removed by Chemical Milling
AE	Simulated SPF Conditioning. As Exposed, 90 min in Air Furnace at either 788 °C, 845 °C, or 885 °C followed by room air cool.
AE + PP	AE with Proposed, reduced Processing – no chemical milling. Visible α case plus material representative of two cleaning cycles is removed by chemical cleaning. This simulates α case removal plus standard cleaning of an SPF part using representative existing processes.
AE + FP	AE with current representative production (Full) Processing, including chemical milling to remove 150% of the visible α case.

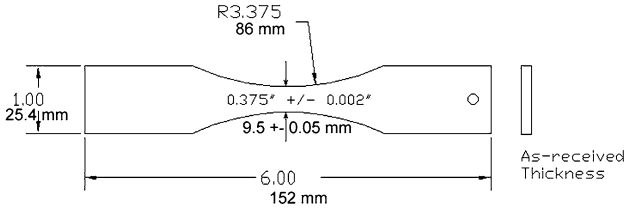

Fig. 3 Constant Amplitude Fatigue Specimen, $K_t = 1.03$

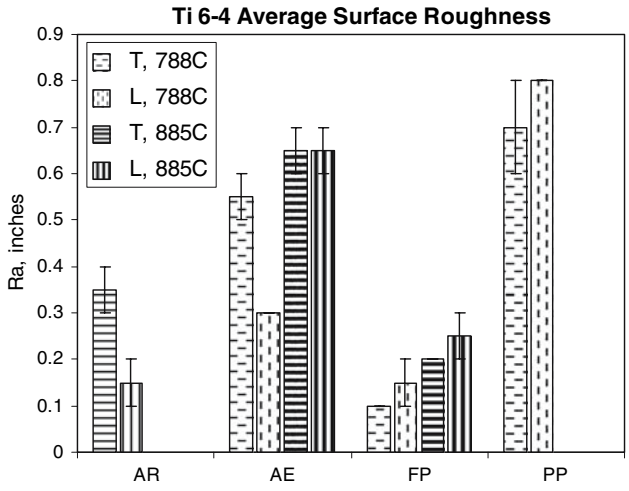

Fig. 4 Average Surface Roughness of Ti 6-4 under Different Conditions

cycling process induces a rougher surface but at the same time eliminates the directional difference.

Average surface roughness values are plotted in Fig. 4. The lowest roughness was seen in the FP (chemically milled) condition (less than 0.020 μm), and only slight differences between the T and L directions are apparent. After the PP post processing, the directional difference is much less than either the as received or as exposed groups, however the surface roughness is greater than the FP group. The surface roughness of the PP and AE groups is similar. It is possible that the less aggressive chemical cleaning solution does not remove the roughness as well as the faster, more aggressive chemical milling process.

Figure 5 shows the datapoints and S-N curves plotted for Ti 6-4 after the 788 °C (1450 °F) conditioning in (a) and the datapoints and curves for Ti 6-4 after 885 °C (1625 °F) conditioning in (b). Both post-processing methods (PP and FP) as well as the as received (AR) and as exposed (AE) conditions

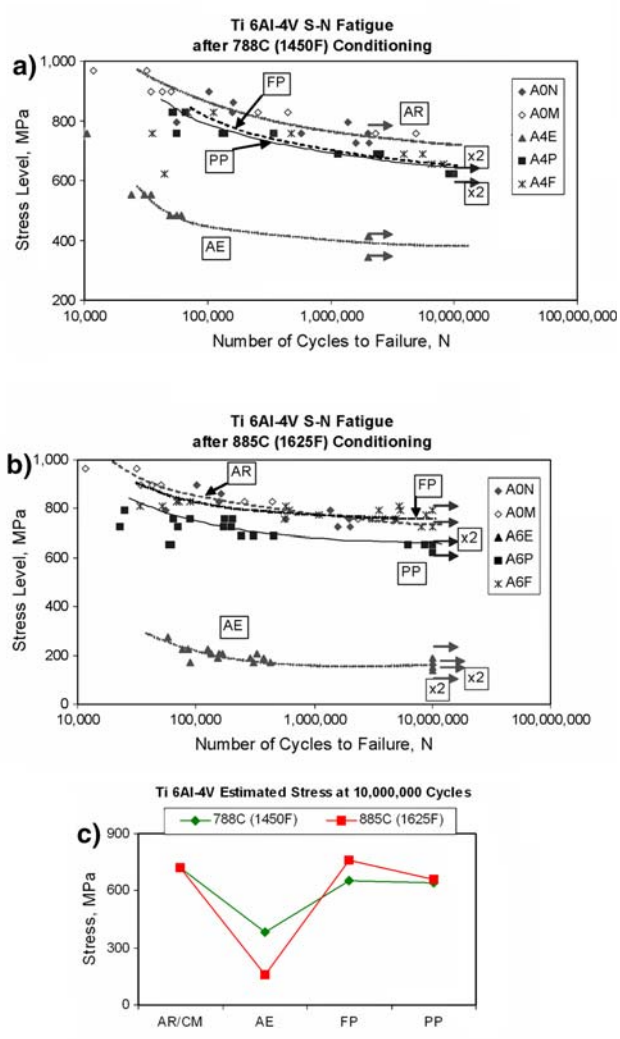

Fig. 5 Ti 6-4 S-N Fatigue Results after (a) 788 °C Conditioning, (b) 885 °C Conditioning, and (c) Estimated Stress at 10 Million Cycles

are represented in these graphs. A single curve (AR) represents the combined A0N and A0M groups. Arrows represent unfailed (run-out) specimens. Several stress levels in each Figure are associated with multiple run-out specimens. These multiples are indicated with an ×2 symbol, indicating that 2 run-outs occurred at that stress level. The graphs of Ti 6Q2 and SP 700 in Fig. 6 and 7 have similar notation.

The curves representing the 788 °C (1450 °F) Ti 6-4 data after both PP and FP post-processing methods are nearly

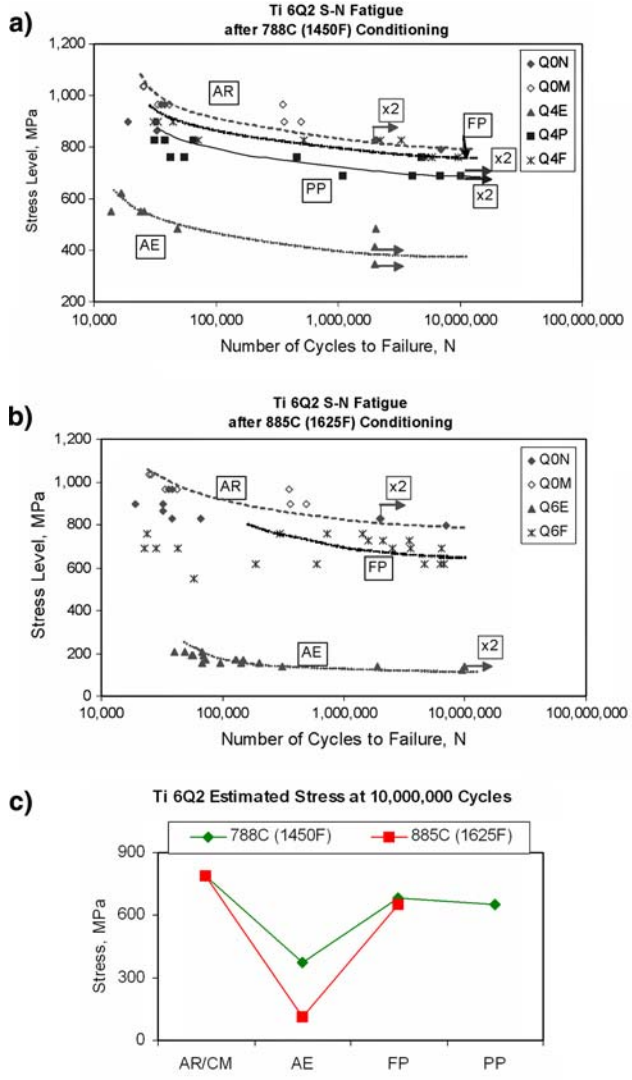

Fig. 6 S-N Fatigue Results for Ti 6Q2 after (a) 788 °C Conditioning, (b) 885 °C Conditioning, and (c) the Estimated Stress Level at 10 Million Cycles

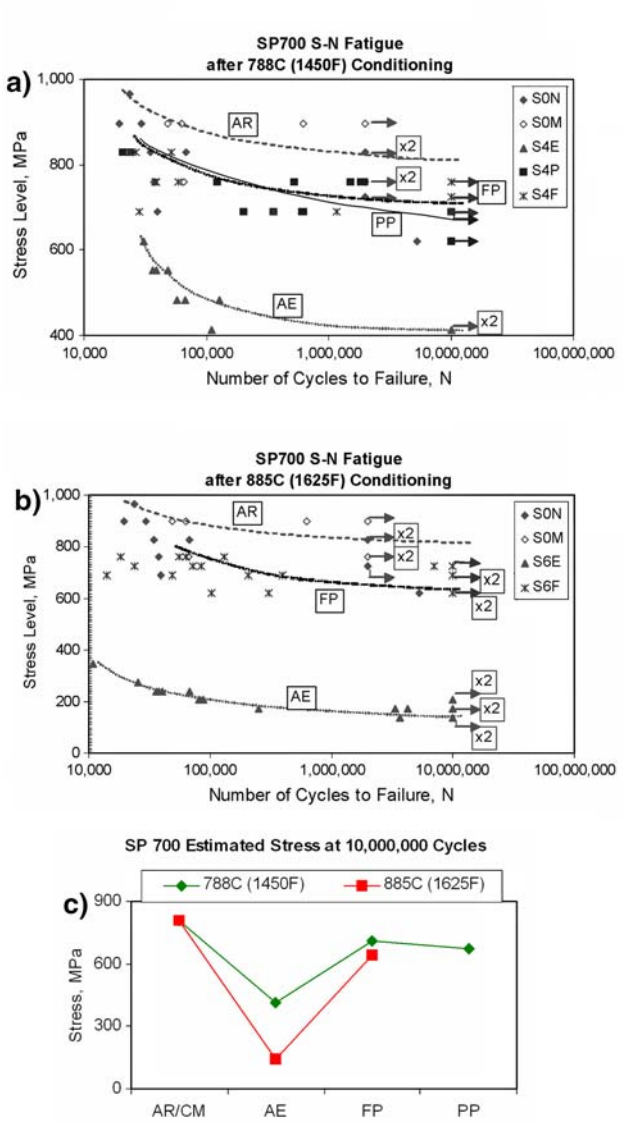

Fig. 7 S-N Fatigue Results for SP 700 after (a) 788 °C Conditioning, (b) 885 °C Conditioning, and (c) Estimated Stress Level at 10 Million Cycles

identical while the AE group is dramatically lower than any of the other groups. The AR group exhibits the best results. After being conditioned at 885 °C (1625 °F), the AR group again has the highest performance although the FP group is nearly as good. The PP group is slightly lower and the AE results are considerably less than half the results of the other groups. Figure 5(c) compares the estimated maximum stress level that will survive to 10 million cycles between the evaluated groups.

Of note in Fig. 5 is that the AE group loses almost 60% of its fatigue strength capacity after 885 °C (1625 °F) conditioning when compared to the 788 °C (1450 °F) AE conditioning and almost 80% when compared to the AR condition. The PP values are the next lowest but much closer to the FP and AR values. After 788 °C conditioning and PP post-processing values for Ti 6-4 material are 98% of the 788 °C conditioned and FP post-processed values and 89% of the AR values. The corresponding values for 885 °C conditioning are 87% and 92%, respectively.

The results for Ti 6Q2 after both 788 °C (1450 °F) and 885 °C (1625 °F) conditioning are shown in Fig. 6(a) and (b). The estimated maximum surviveable stress levels at 10 million cycles for each condition are estimated from these graphs and are shown in Fig. 6(c). Once again, the AR values are the highest and the AE values are the lowest at 47% and 14% of AR after 788 °C and 885 °C conditioning, respectively. The PP post-processed Ti6Q2 (788 °C conditioned) is nearly the same as (4.4% lower) the FP post-processing. After 885 °C (1625 °F) conditioning, the FP specimens drop to 82% of the AR results.

The results for the SP 700 material are presented in Fig. 7(a), (b), and (c). The material conditioned to the 788 °C (1450 °F) simulated SPF cycle was consistently lower in maximum stress level for the equivalent number of cycles after both post-processing methods, 12% and 17% for FP and PP, respectively, as compared to the as received material. After the 885 °C (1625 °F) SPF conditioning cycle, the FP post-processing method produced 21% lower results than the as received material. In both cases, the AE material is well below any of the other cases, 51% and 17% of AR after the 788 °C and 885 °C conditioning cycles. After the 885 °C conditioning cycle, the

estimated maximum surviveable value at 10 million cycles is 34% of the value of SP 700 material AE to 788 °C (1450 °F).

Fatigue cracks initiate in a number of different locations. Figure 8 identifies the location nomenclature and Fig. 9(a), (b), and (c) present the data in graphic format for the respective alloys Ti 6-4, Ti 6Q2, and SP 700. The initiation sites were identified visually under low magnification. The numbers shown in parenthesis with each condition along the *x*-axis represent the total number of specimens in each condition. Not included in these numbers are the specimens that failed at defects, in the grip area, and the run-out specimens. Several of the specimens had multiple distinct initiation sites. The AE specimens had so many initiation sites, it was difficult to observe distinct initiations.

In all three alloys, the AR specimens had the highest % of cracks initiated at corners; 60%, 85%, and 80% for Ti 6-4, Ti 6Q2, and SP 700, respectively.

A typical fatigue fracture face showing the crack origin is shown in Fig. 10(a). This Ti 6-4 specimen was recorded with a Face initiation site. The areas identified as "Origin" and "A1" are shown at a higher magnification in Fig. 10(b) and (c), respectively. "Origin" exhibits the typical jumbled appearance and fine striations of a fatigue crack origin. "A1" shows striations that are characteristic of a fatigue crack growing by crack opening and closing and are found in the smooth area of the fractured face. In this specimen, the lack of beach marks indicates that the crack growth was smooth and uninterrupted.

Figure 11(a) illustrates a fatigue fracture initiating at the corner of the specimen in the lower right of the photograph. An

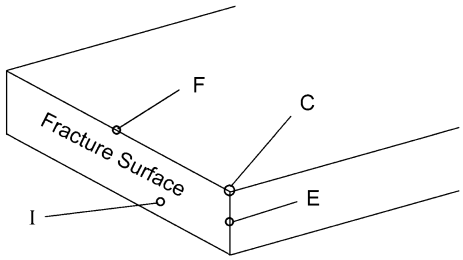

Fig. 8 S-N Fatigue Crack Origin Key. Locations F = Face, C = Corner, E = Edge, and I = Subsurface

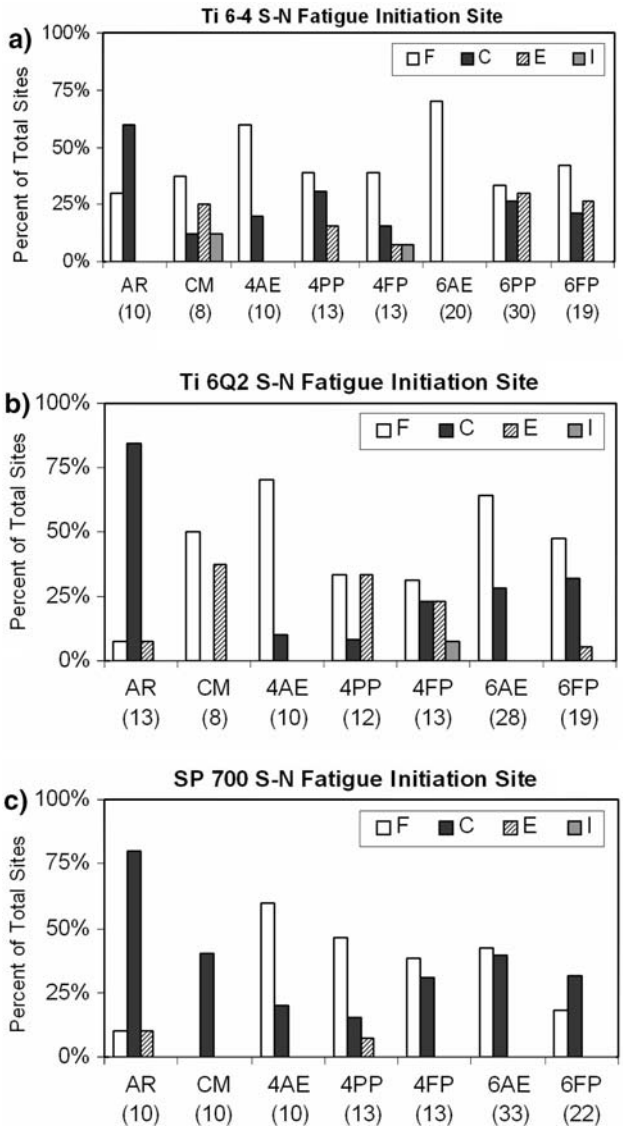

Fig. 9 Distribution of Crack Initiation Sites on (a) Ti 6-4, (b) Ti 6Q2, and (c) SP 700 S-N Specimens

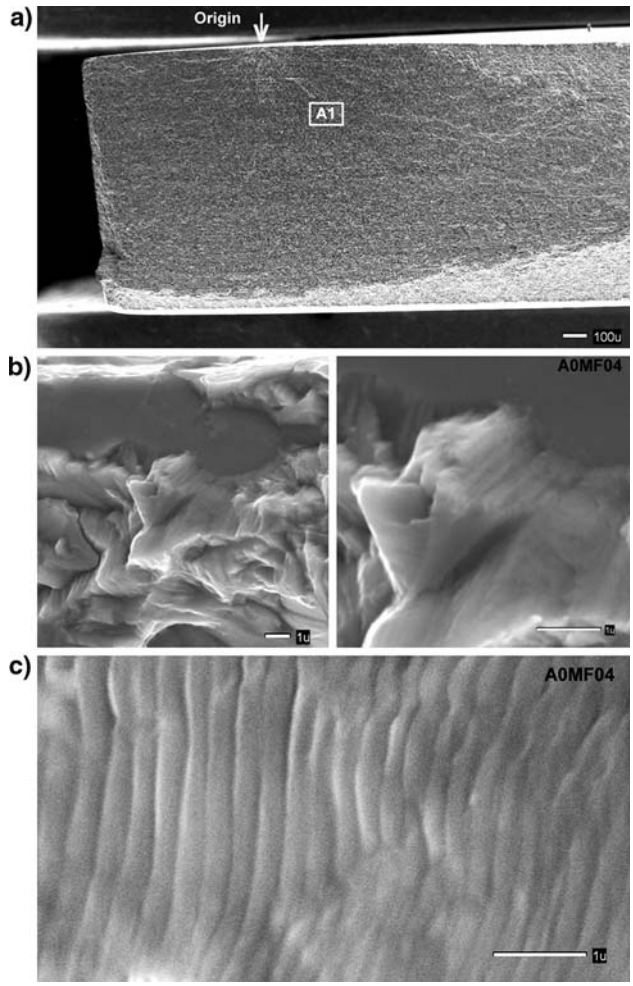

Fig. 10 (a) Fatigue Failure Origin on Ti 6-4 Specimen, (b) SEM Fatigue Fracture Surface, Near Failure Origin, (c) Fatigue Striations at Location A1

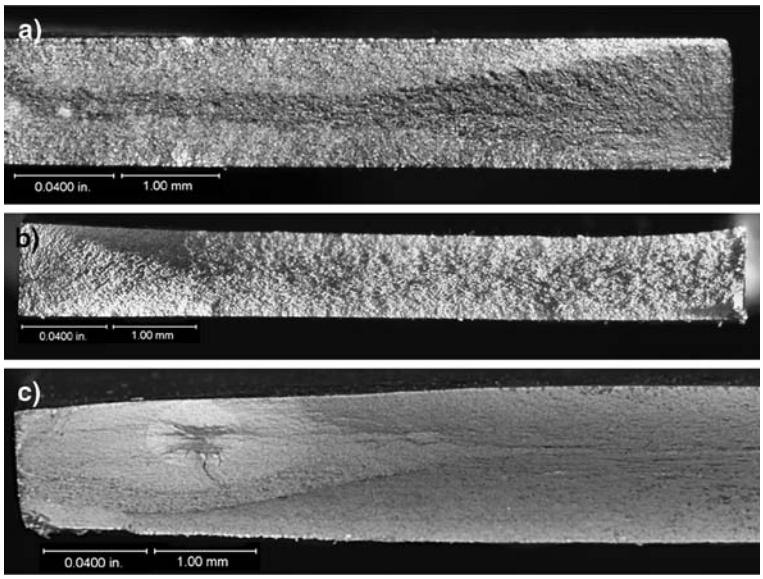

Fig. 11 (a) Corner Crack Origin (lower right) on Ti 6-4 Material after 788 °C Conditioning and Full Post Processing, (b) Edge Crack Origin (middle left) on Ti 6-4 after 885 °C Conditioning and Full Post Processing, (c) Interior Crack Origin (middle left) on Ti 6Q2 Material after 788 °C Conditioning and Full Post Processing

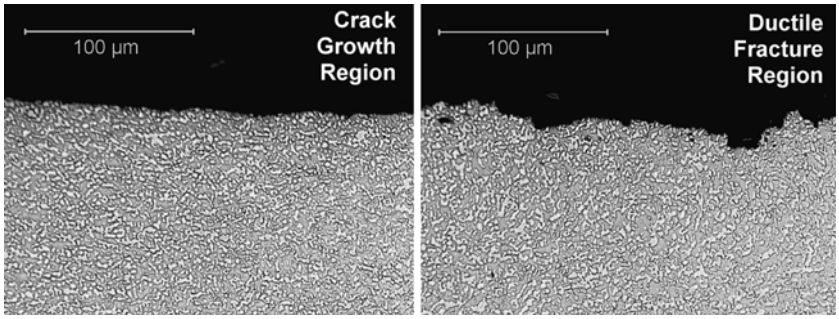

Fig. 12 Fracture Along Face of Specimen in Crack Growth and Ductile Fracture Regions, SP 700 Material

edge crack origin is shown in Fig. 11(b) on the left-hand side of the photograph. The crack originated in the dark area of the specimen just below center of the left edge.

Figure 11(c) shows an example of a subsurface (interior) crack initiation. This type of crack initiation is usually associated with a flaw in the material but has been associated with high cycles/low stress fatigue in titanium. The specimen also shows evidence of beach marks, the areas of different shades around the crack initiation site. Beach marks indicate that the crack growth was interrupted during the testing.

Figure 12 shows the crack growth surface at the face of the specimen. The crack origin area where the crack is progressing during load cycling is shown on the left. It is characterized by a smooth line, nearly perpendicular to the loading direction. The area on the right is in the ductile fracture area, where the specimen was overloaded and fractured. The fracture is characterized by an irregular path along the face of the specimen.

4. Discussion

None of the PP material met the AR properties in S-N fatigue within 5% and the surface roughness values did not seem to predict the differences in S-N fatigue properties. It is possible that some undetected elevated oxygen is present in the PP material, however, other possibilities that were not studied in this investigation include material response to the heat cycle such as microstructural ordering, precipitates, and textural changes.

For practical structural design purposes, the specimen configuration would be designed with a stress concentration factor approximately equal to a hole in the material, $K_t = 3.0$ (Ref 4). The specimen configuration with a K_t of 1.03 used in this investigation provides useful data for comparison purposes, however, most likely would not be used in structural design calculations because most structure contains holes for fasteners, conduits, fuel flow, etc. Data from specimens with a K_t of 3.0, representing a hole, is plotted with the Ti 6-4 data in Fig. 13. This curve shows that although the post-processed material has lower properties than the AR material, it is well in excess of the $K_t = 3.0$ data and would be equivalent to the AR Ti 6-4 for design purposes. Additional testing is warranted with K_t of 3.0 or greater to determine whether the material subjected to SPF is indeed equivalent to the AR material of like configuration, and to investigate the actual cause of the reduced properties.

In the S-N fatigue results it is obvious that as exposed material has a very low life compared to as received material, or any of the post-processed material. This result is consistent

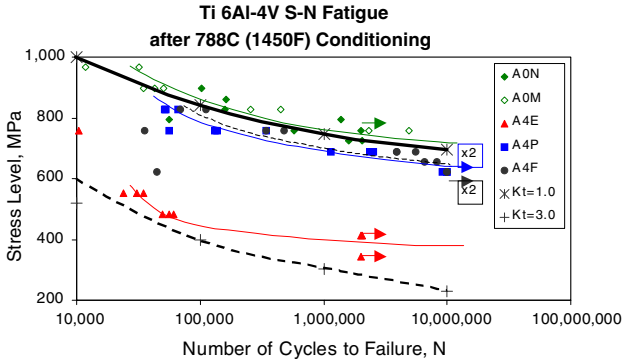

Fig. 13 Ti 6-4 S-N Fatigue Results Relative to K_t of 1.0 and 3.0

across all three alloys after all three temperature-conditioning cycles, and consistent with published results. However, there is a considerable drop in S-N fatigue life in the as exposed condition as the conditioning temperature increases. This result was not previously documented.

Crack initiation sites were identified in various locations on the specimen surfaces. Corners were the dominant crack initiation sites only in the as received specimens, which were the first groups to be cycled. These specimens also had many failures at relatively low number of cycles for the applied stresses. Face initiation sites were the most numerous in all of the other conditions in all three alloys. Corners would normally be considered the highest stress concentration in the dogbone specimen. The major location of crack initiations changing from the corners on the AR specimens to the face on the rest of the specimens indicates that either the corner stress concentration was reduced by the processing or stress concentrations were increased on the specimen faces.

5. Summary

Some type of post processing is necessary to restore S-N fatigue properties. After 885 °C (1625 °F) simulated SPF conditioning, nearly full life is restored with the FP post processing in Ti 6-4 material. In all other cases the post processing did not restore full as received properties. Surface roughness varied between the material conditions and did not seem to predict the high-cycle fatigue behavior.

In high-cycle fatigue, the proposed post-processing method is equivalent to the full post-processing method in all three materials conditioned at 788 °C (1450 °F). In the single case that compares the two post-processing methods after 885 °C (1625 °F) conditioning, the Ti 6-4 S-N fatigue results were slightly lower for the proposed method than the full post-processing method. In all cases evaluated (all three materials after 788 °C conditioning and Ti 6-4 after 885 °C conditioning), the material subject to simulated SPF conditioning had slightly lower life than the as received material, however, experienced longer fatigue life than published data for material with a stress concentration factor of 3.0.

6. Conclusions

The proposed processing method is as effective at restoring strength and fatigue properties as the full, current post-processing method after simulated SPF conditioning at 788 °C.

A slight reduction in S-N fatigue properties is evident after simulated SPF processing regardless of post-processing method.

Results from all post-processed material exceed published results for a $K_t = 3.0$.

High-cycle fatigue failure modes are consistent with literature data.

References

1. F.S. Pitt, "Influence of Time, Temperature and Alloy on Oxygen Absorption in SPF Titanium," Master's thesis, University of Washington, 2000
2. J.A. Ruppen, C.L. Hoffmann, and V.M. Radhakrishnan, The Effect of Environment and Temperature on the Fatigue Behavior of Titanium alloys, *Fatigue, Environment and Temperature Effects*, J.J. Burke and V. Weiss, Eds., Plenum Press, 1980, p 265–300
3. D.J. Dorr, "Built-Up Low Cost Advanced Titanium Structures," 1979, Materials Laboratory, Air Force Wright Aeronautical Laboratories, AFWAL-TR-79-3146, 1979, p 200
4. D.B. Lanning, G.K. Haritos, and T. Nicholas, High Cycle Fatigue Behavior and Notch Size Effects in Ti 6Al-4V, in *Mechanical Behavior of Advanced Materials*, D.C. Davis, A.M. Sastry, M.L. Dunn, an A.K. Roy, Eds., Anaheim, CA, The American Society of Mechanical Engineers, 1998, p 19–25